
Proceedings of the Sixth International Conference on
Railway Technology: Research, Development and Maintenance
Edited by: J. Pombo
Civil-Comp Conferences, Volume 7, Paper 3.7
Civil-Comp Press, Edinburgh, United Kingdom, 2024
ISSN: 2753-3239, doi: 10.4203/ccc.7.3.7


# Numerical Modelling of Partially Loaded Freight Train Entering a Tunnel

**Z. Liu and D. Soper**

**School of Civil Engineering, University of Birmingham**
**United Kingdom**

## Abstract

The large gaps between wagons and loaded goods, influence the pressure wave pattern generated by it passing through a tunnel. The accurate resolution of separation regions at the head of the blunted containers, and at unloaded gap sections is essential for precise predictions of pressure magnitude. Achieving this accuracy demands exceptional mesh quality, significant computational resources, and the careful selection of numerical models. This paper evaluates various numerical models to capture these complexities in separation regions. A 1d programme is developed to calculate the pressure wave generated by freight loco entering a tunnel, and is further extended to consider the discontinuities of the train body by implementing new mesh system and boundary conditions into the 1d programme. The results obtained from the 1d programme are validated against large eddy simulation data. A parameterisation study for different loading configurations improves program adaptability, and the relationship between predetermined parameters and gap length is investigated. This research bridges the gap in freight train tunnel aerodynamics, offering a versatile 1d computational tool for accurate pressure wave prediction.

**Keywords:** freight train, computational fluid dynamics, one-dimensional numerical method, train/tunnel aerodynamics, large eddy simulation, vehicle aerodynamics.

# 1 Introduction

Numerous studies have been conducted to consider the aerodynamics of trains in tunnels [1]. However, the majority has focused on passenger trains due to the speed at which these vehicles travel. Although freight trains travel at general slower speeds to passenger rolling stock, the shape of a freight train typically looks very different to that of a passenger train [2], for which these 1d studies have been traditionally undertaken.

As a freight train passes through a tunnel, it generates a unique characteristic set of pressure wave patterns that different from passenger trains, due to the blunted nose shape of freight trains, and the loading configurations of goods carried. The influence of the blunted nose on pressure waves have been numerically and experimentally studied by Iliadis [2]. The separation bubble generated at blunted train head increases the effective blockage area, of which has been investigated by doing parameterisation study and implemented into a modified 1d code [3]. Moreover, the front face of the container after large gaps generates subsequent pressure waves, and thus influence the pressure wave pattern during train body enters the tunnel.

However, the influence of the train body on pressure variation is calculated using frictional coefficient, train length and cross-sectional area in traditional 1d method [4], which is inappropriate for a freight train, due to nature of the wagon and load formations. Therefore, traditional method is incapable of predicting the series of pressure waves generated by the big gaps between containers loaded onto intermodal freight trains, as the individual wagon/container enters into the tunnel, especially for partially loaded freighted trains.

The flow characteristics observed at the gap of partially loaded containers closely resemble those of a platoon of bluff bodies. Research efforts have been dedicated to studying the wake interference phenomenon (buffeting) arising from the arrangement of two or more bluff bodies with varying sizes and gap lengths. Notably, havel [5] conducted experimental investigations on surface-mounted cubes with varying the gap length, under a Reynolds number of 22,000. Three regimes are summarised and briefly described as Bi-stable Regime, Lock-in Regime and Quasi-isolated Regime.

Similar flow regimes are identified and analysed for various upstream and downstream dimensions of different bluff bodies [5-7]. While these studies offer valuable reference data for sharp-edged three-dimensional objects like wagons, it should be noted that the Reynolds numbers considered in most of these studies are significantly lower than those encountered in train flows.

The primary objective is to bridge these gaps by evaluating various numerical models and their efficacy in addressing aerodynamic challenges posed by freight trains passing through tunnels. Additionally, the research endeavors to develop an enhanced 1d program capable of accurately simulating the pressure waves generated by freight trains, utilising the proposed novel model.

# 2 Methodology

In this section we briefly introduce the large eddy simulation (LES) numerical model and the modifications made on the 1d model. More details of the 1d programme can be referenced by Zhen[3].

## 2.1 LES model

In the LES methodology, a filter is employed to distinguish between the larger scales and smaller ones. Consequently, all variables such are divided into grid and sub-grid components. Upon filtering the variables within the compressible Navier-Stokes equations, the resulting equation at the instantaneous filtered level manifests in the subsequent equations. A Wall-Adapting Local Eddy-Viscosity (WALE) model is adopted for the subgrid-scale (SGS) model in this study. Previous research illustrate that the WALE model performs well in resolving complex flows, including those with separation regions benchikh2019turbulent, such as the flow created about the bluff freight train.

To reduce the error caused by discretisation, a second-order upwind scheme is used for the discretisation of the convection diffusion terms iliadis2020numerical. The bounded central differencing scheme is used for the discretization of the convection terms to ensure the accuracy and stability of the simulation. The relevant control equations are solved using the CFD software Fluent based on the finite volume method, and a PISO pressure-velocity coupling method is also adopted. The time derivative is discretized using the bounded second-order implicit scheme for the unsteady calculation. The time step $\Delta t$ is set as $4 \times 10^{-5}$, estimated by CFL$\leq$1 ($CFL = \Delta t \cdot v/\Delta x_{\min}$, where $v$ is the train operating speed (33.5m/s) and $\Delta x_{\min}$ is 0.0015m in this paper).

## 2.2 Modification on the 1d code

This chapter introduces the modified mesh system of a locomotive with a partially loaded container entering a tunnel, as illustrated in Figure 2, in which the grid in the annulus space ($X_2$) is based on the train as the frame of reference. The annulus space around the train is further divided into sub-meshes by the ends of the gap between containers. The flow in each sub-mesh system is solved using MOC method based on the corresponding different physical parameters (length, perimeter, cross-sectional area, etc) and the flow connecting different sub-meshes is solved by the boundary conditions illustrated in the following paragraph. Through this approach it can be seen from Figure 2 that although there are discontinuities along the train body, it doesn't have to separate the mesh at the annulus space when the train enters the tunnel, which avoids the excessive extending and extracting mesh when the reference frame is based on the ground.

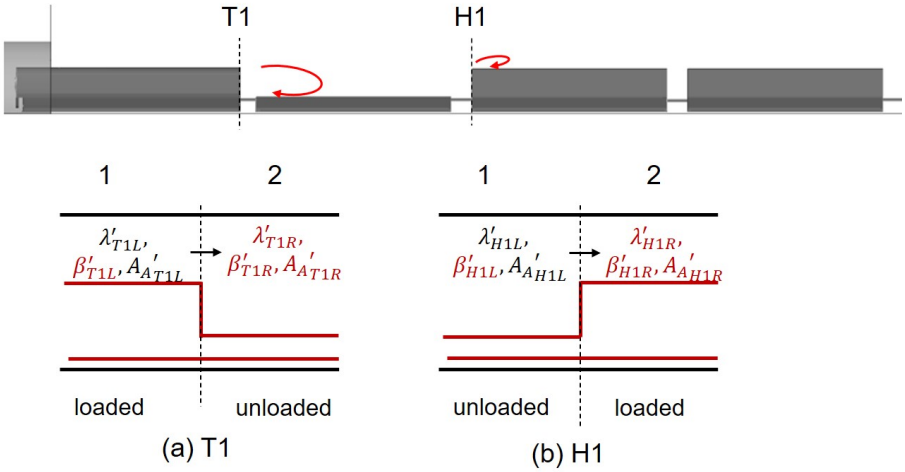


Figure 1: New boundary condition at the ends of containers for a partially loaded train.

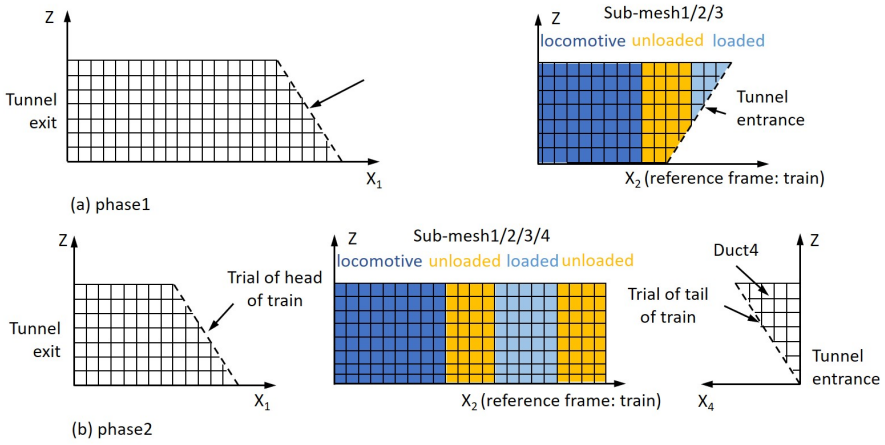


Figure 2: Mesh system for a partially loaded train.

$$(\lambda'_{T1L}+\beta'_{T1L})^2-(\lambda'_{T1R}+\beta'_{T1R})^2+\frac{2}{\kappa-1}\left[(\lambda'_{T1L}-\beta'_{T1L})^2-(\lambda'_{T1R}-\beta'_{T1R})^2\right]=0 \tag{1}$$

$$(\lambda'_{T1L}-\beta'_{T1L})^2(\lambda'_{T1L}+\beta'_{T1L})^{\frac{2}{\kappa-1}}\left(\frac{A_{A_{T1R}}}{A_{A_{T1L}}}\right)^{\frac{2\kappa}{\kappa-1}}- \frac{E_{T1R}}{E_{T1L}}(\lambda'_{T1R}-\beta'_{T1R})(\lambda'_{T1R}+\beta'_{T1R})^{\frac{2}{\kappa-1}}=0 \tag{2}$$

$$\frac{A_{A_{T1R}}}{A_{A_{T1L}}} = \left( 1 + \frac{\frac{2\kappa}{(\kappa-1)^2}\left(\frac{\lambda'_{T1R}-\beta'_{T1R}}{\lambda'_{T1R}+\beta'_{T1R}}\right)^2 \zeta_{T1}}{\left[1+\frac{2}{\kappa-1}\left(\frac{\lambda'_{T1R}-\beta'_{T1R}}{\lambda'_{T1R}+\beta'_{T1R}}\right)^2\right]^{\frac{\kappa}{\kappa-1}}} \right)^{\left(\frac{\kappa-1}{2\kappa}\right)} \tag{3}$$

Note that the cross-sectional area $E_{T1L}$ is the effective cross-sectional area considering the separation at the end of the loaded container. The effective cross-sectional area at the gap is also used to calculate the pressure loss at train tail,

$$\zeta_{T1} = (\frac{(E_{Con} - E_{Gap})}{E_{TU} - E_{Con}})^2 \tag{4}$$

in which $E_{Con}$ is the cross-sectional area of the loaded container and $E_{Gap}$ is the effective cross-sectional area of the gap. Apart from the equations. $1 \sim 3$, a characteristic equation is also needed to solve the four unknown variables. Equations are solved using Newton Raphson method. For the equations to solve the flow from the unloaded region to loaded region, the subscript T1 is substituted by H1. Furthermore, due to the sharp front edge of the container, a separation bubble forms when then air flows over from the gap in front. The size of the separation bubble and the pressure loss coefficient changes with the distance of the gap. Details of the relationship between the parameters which need to be determined and the gap size are discussed in the following sections.

## 2.3 Parameters

In order to facilitate and ease comparison between cases considered, Table 1 have been constructed as a point of reference for numerical simulations in the results and discussion regarding to different loading configurations separately. Case 1 to 3 serve as the references cases for investigating various loading configurations. They evaluate the effectiveness of LES and URANS models in simulating the pressure wave generated when partially loaded containers enter a tunnel. These results form the basis is used for constructing the physical model in the 1d program and validating the outcomes of the modified 1d code. Subsequently, Cases 4 to 6 focus on a parameterization study of loading configurations. This involves analysing how the unloaded gap impacts the effective cross-sectional area within the gap and the size of the separation bubble formed at the leading edge of the trailing container. The insights gained from this parameterization study are then incorporated into the 1d program (Case 7) to simulate the pressure wave generated when a freight train entering a tunnel, where the first carriage is fully empty.

| Case | Geometry | | Operating Condition | Numerical Model | Description |
|---|---|---|---|---|---|
| | Train | Tunnel | | | |
| 1 | Class 66 with 4 33% loaded containers | 45 $m^2$ | Tunnel | 1d model | Reference |
| 2∼3 | Class 66 with 4 33% loaded containers | 45 $m^2$ | Tunnel | LES | Reference |
| 4∼6 | Class 66 with 2 containers, with the first container fully loaded/20/40/60 foot gap | 45 $m^2$ | Inside tunnel (steady) | LES | Parameterisation on Loading configurations |
| 7 | Class 70 locomotive | 45 $m^2$ | Tunnel | 1d model | Validation |

Table 1: Summary of loading configurations.

# 3 Mesh

Since the prediction of the separation bubble is very sensitive to the mesh quality, and subsequently the numerical model chosen, the whole computational domain is divided by a structured mesh to increase the overall mesh quality krajnovic2002large, iliadis2020numerical. The entire computational domain has been meticulously divided into hundreds of hexahedral block regions. In contrast to automatically generated meshes controlled by predefined parameters, the utilization of a manually crafted structured mesh allows for precise control over the quality of each element. This approach mitigates the occurrence of poor-quality meshes, particularly at sharp edges or areas with significant curvature changes. Remarkably, more than 99.5% of the mesh exhibits a skewness quality lower than 0.54. Moreover, mesh at the region that forms after the flow separates over the leading edges of the train head is refined further to resolve all motion down to the inertial subrange. Similarly for partially loaded freight train, the mesh at the unloaded gap is also refined. For the case of freight train with 4 33% loaded containers, the blocking structure and the mesh around the train are shown in Figure 3 and 4.

# 4 Results

## 4.1 Reference Case

In order to establish an initial comprehension of the flow field and to derive essential parameters for input into the 1d code, a reference case featuring a 33% loaded intermodal container freight train entering a tunnel is subjected to numerical investigation. Subsequently, the parameters derived from these simulations are integrated into the modified 1d code to validate the suitability of the proposed algorithms.

Given that the locomotive and tunnel geometries remain consistent with the reference case detailed in Zhen[3], the parameters utilised in the 1d code for the locomotive (Class 66 for the initial reference design case) and the tunnel adhere to those presented in Zhen[3]. Notably, since the container cross-sectional area (without considering the separation bubble region) is marginally smaller than that of the locomotive, es-

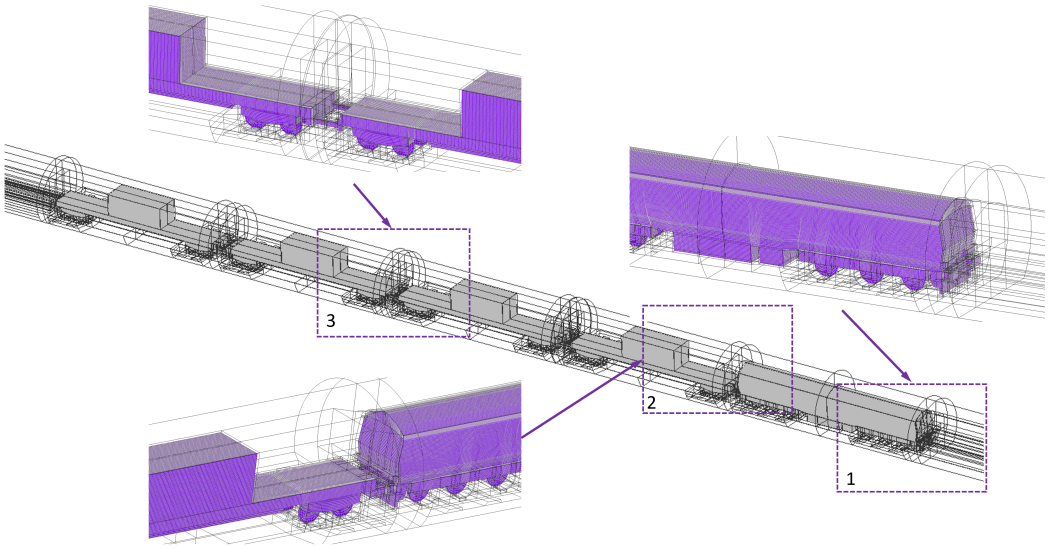


Figure 3: The blocking structure around the 33 % partially loaded freight train

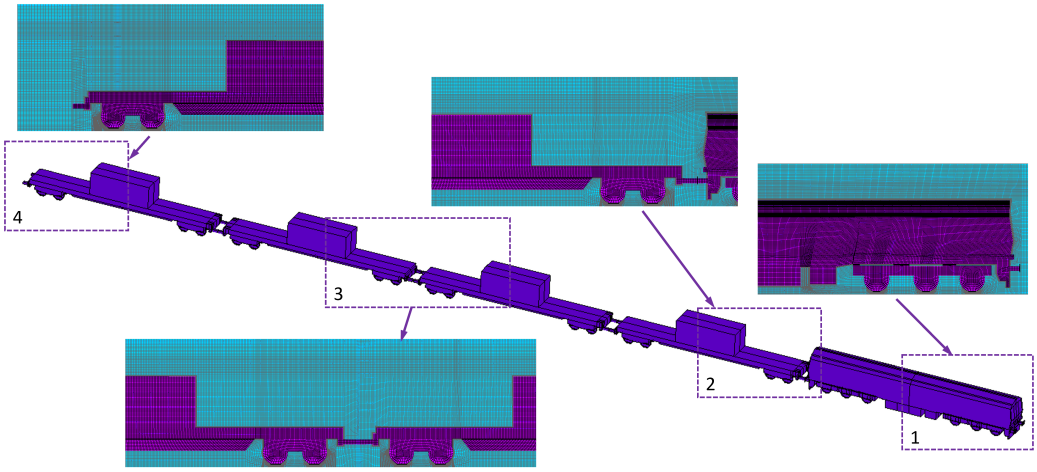


Figure 4: Mesh size and distribution around the 33 % partially loaded freight train

timated to be approximately 10 $m^2$ in the code. Besides, given that the relationship between separation bubble size and the pressure rise induced by pressure waves during train tunnel entry has been previously established and analysed in previous research, a best-fit method [vardy1999estimation] is employed to deduce the parameters governing the separation bubble sizes for the containers after the 33% $L_{\text{CAR}}$ and 66% $L_{\text{CAR}}$ gaps. These parameters are mainly utilised for validating the feasibility of the proposed algorithms in the methodology section, while more comprehensive analysis

will be conducted in subsequent sections through the examination of mean flow fields from LES simulations in freight trains featuring diverse loading configurations. The comparison of pressure variation at 2/4/8/16 m at tunnel surface between the LES and 1d numerical result are presented in Figure 5. Results show that the 'step-like' pressure rise caused by the unloaded and loaded container entering the tunnel calculated using the modified 1d model fits well with LES simulation.

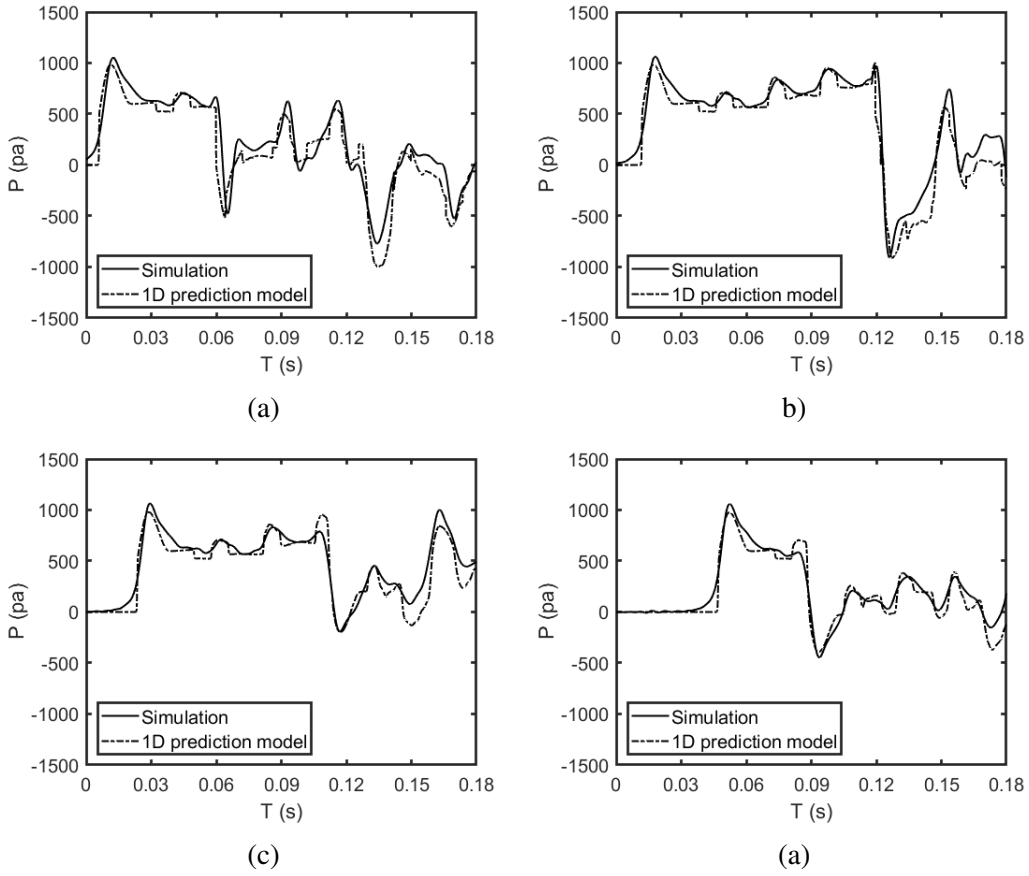


Figure 5: Comparison of pressure history curve obtained from 1d result and LES simulation (a) 2 m (b) 4 m (c) 8 m (d) 16 m.

## 4.2 Parameterisation Study

Parameterization study is carried out by simulating 33%/66%/100% unloaded intermodal container freight train entering the tunnel. Figure 6 display the mean velocity distribution and streamlines of container 1 for each loading configuration separately. A consistent observation across all loading configurations is the separation of the boundary layer at the locomotive's end, resulting in large vortices. The recirculation wake length is about 0.25 times the container length, shorter than the smallest gap size (0.33 $L_{\mathrm{CAR}}$). In cases with gap lengths of 0.33 and 0.66 $L_{\mathrm{CAR}}$, the trailing container is positioned at the wake reattachment zone, causing air obstruction and forming a backflow

region. In the 0.33 $L_{\mathrm{CAR}}$ gap case, this backflow region connects with and influences the wake recirculation, resulting in longer vortex length and higher Turbulent Kinetic Energy (TKE).

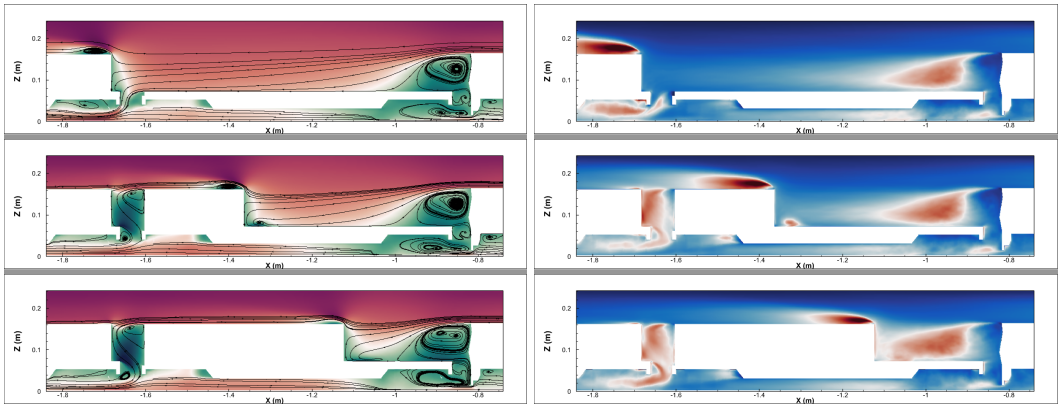

(a) b)

Figure 6: Velocity field of the second container at contour Y=0 m (a) mean $u$ and streamline (b) TKE.

In order to build the model to calculate the effective blocakge area, the flow motion over and inside the gap between two containers can be characterised into three parts, and a diagram visualising these regions is illustrated in Figure 7.

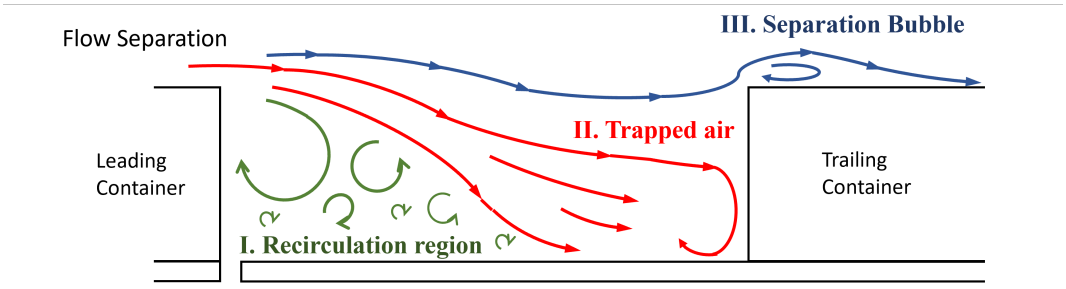


Figure 7: Diagram of flow characteristics inside the gap.

1. The recirculation region dominated by large wake vortices generated from the separation of the boundary layer from the leading container.
2. The air flow downwash from the tail of the leading container, blocked by the trailing container, forming a recirculation in front of the trailing container and moving with the train as trapped air in the gap.
3. The outer part of the air can escape the gap and flow over the trailing container, forming a separation bubble region behind the sharp leading edge of the trailing container.

It is important to highlight that both region I and II contribute to the increase in the effective cross-sectional area of the unloaded part of the train. The effective blockage areas for gap lengths of 33 % and 66 % $L_{\text{CAR}}$ were determined using the best fit method, resulting in values of $0.85 \times E_{\text{container}}$ and $0.7 \times E_{\text{container}}$ respectively. Additionally, for a fully loaded freight train (gap length is zero), the effective cross-sectional area equals $1 \times E_{\text{container}}$. Assuming the upper edge of the trapped air flow trajectory is approximately a straight line, indicating an approximately linear relationship between the gap length and the effective blockage area, the effective blockage area at a 100 % $L_{\text{CAR}}$ gap is estimated to be approximately $0.55 \times E_{\text{container}}$. This parameter will be further incorporated into the 1d programme to simulate a freight locomotive with four containers (the first container being fully unloaded) entering a tunnel.

Region III represents the separation bubble region around the trailing container, and its size significantly impacts the pressure wave rise when the container enters the tunnel, especially for sufficiently long gaps where the bubble size cannot be neglected. The separation bubble model for the containers is similar to that for the locomotive as illustrated in Zhen [2]. Although the dimensions differ, the methodology and data processing procedures remain the same.The relationship equations among the heights of separation bubbles at the top and side of the container and the percentage gap length are consolidated in Figure 8.

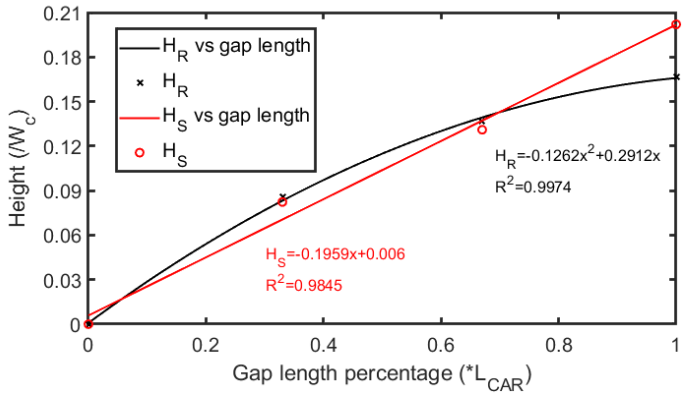


Figure 8: The relationship between separation bubble height and the percentage of unloaded container.

Incorporating the predetermined parameters $r_{b_C}$ and the effective blockage area for a freight train with the first carriage fully unloaded into the 1d programme, the pressure history curves for measuring points at 2 m, 4 m, 8 m, and 16 m inside the tunnel are illustrated in Figure 9. With the integration of these parameterization models into the modified 1d programme, it is evident that the programme can predict the pressure wave patterns generated by freight trains with diverse loading configurations.

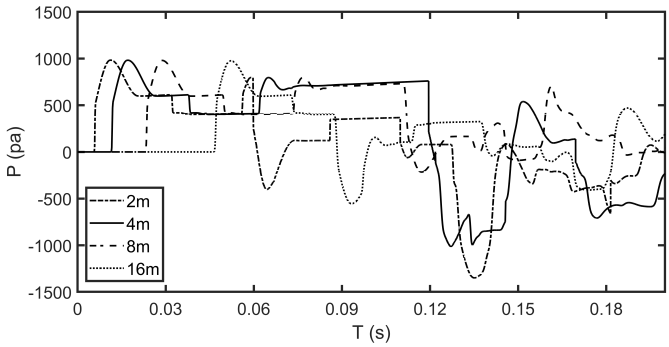


Figure 9: Pressure history curve of a freight locomotive with four containers (first container unloaded) entering a tunnel predicted by redeveloped 1d programme.

# 5 Conclusions

A thorough assessment was conducted to ascertain the suitability of different numerical models for accurately simulating the pressure waves generated as a partially loaded freight train enters a tunnel. Subsequently, a redeveloped 1d programme was introduced, enhancing its capabilities to simulate the discontinuities in the train body and consequent pressure wave alterations induced by partial loading. Furthermore, a parameterization study was executed, involving the relationship between predetermined parameters and gap length, through LES simulations. In summary, the study in this chapter yielded several noteworthy contributions,

(a) The 'step-like' increase in pressure rise ($\Delta p_{fr}$) resulting from the entry of a partially loaded freight train into the tunnel is linked to the compression and expansion pressure waves produced by the abrupt area change as unloaded gaps enter the tunnel.

(b) The flow pattern within these gaps can be categorised into three regions:

  (i) The recirculation region, dominated by large vortices separated from the leading container.

  (ii) The airflow down-wash from the leading container.

  (iii) The outer airflow passing over the trailing container, forming a separation bubble.

(c) A redeveloped 1d program has been coded, introducing a new mesh system and new boundary conditions. The program's ability to predict the pressure rise caused by a 33% partially loaded container entering a tunnel has been validated by comparing its results with LES simulations.

(d) As the unloaded gap length increases, the effective blockage area of the gap decreases. Furthermore, the air velocity in front of the trailing container increases with longer gap lengths, approaching the train speed. This generates a larger separation bubble where the air flows over the trailing container. These parameters have been numerically studied.

# References


[1] I. Panagiotis, et al., "Numerical simulations of the separated flow around a freight train passing through a tunnel using the sliding mesh technique", Proceedings of the Institution of Mechanical Engineers, Part F: Journal of Rail and Rapid Transit 234.6, 638-654, 2020.

[2] I. Panagiotis, et al., "Experimental investigation of the aerodynamics of a freight train passing through a tunnel using a moving model", Proceedings of the Institution of Mechanical Engineers, Part F: Journal of Rail and Rapid Transit 233.8, 857-868, 2019.

[3] Z. Liu, et al., "Numerical investigation of the slipstream characteristics of a maglev train in a tunnel", Proceedings of the Institution of Mechanical Engineers, Part F: Journal of Rail and Rapid Transit, 237.2, 179-192, 2023.

[4] J. A. Fox, R. E. Vardy, "The generation and alleviation of air pressure transients in tunnels", Tunnels & Tunnelling International, 5.6, 1973.

[5] B. Havel, H. Hangan, and R. Martinuzzi, "Buffeting for 2D and 3D sharp-edged bluff bodies", Journal of Wind Engineering and Industrial Aerodynamics, 89.14-15, 1369-1381, 2001.

[6] H. Hangan, and B. J. Vickery, "Buffeting of two-dimensional bluff bodies", Journal of Wind Engineering and Industrial Aerodynamics, 82.1-3, 173-187, 1999.

[7] M. M. Zdravkovich, "Review of flow interference between two circular cylinders in various arrangements", 618-633, 1977.